

# Contraintes Résiduelles dans les Billettes d'Aluminium : Mesures par Diffraction de Neutrons et Simulation Thermomécanique

J.-M. DREZET<sup>a</sup>, A. EVANS<sup>b</sup> et Th. PIRLING<sup>b</sup>

a. Ecole Polytechnique Fédérale de Lausanne (EPFL), LSMX, station 12, CH-1015 Lausanne

b. Institut Laue-Langevin (ILL), 6, rue Jules Horowitz, F-38042 Grenoble

## Résumé :

*Les contraintes internes qui apparaissent dans les billettes d'aluminium produites par coulée semi-continue trouvent leur origine dans le différentiel du chemin thermomécanique en cœur ou en surface de la billette et posent de sérieux problèmes de sécurité lors de la découpe. Un modèle thermomécanique de la coulée semi-continue a été validé en termes de contraintes résiduelles, ces dernières étant mesurées par diffraction des neutrons. Les composantes radiales, orthoradiales et axiales du tenseur des contraintes ont été mesurées le long du rayon d'une billette de diamètre 320 mm.*

## Abstract:

*The internal stresses that are generated during casting of aluminium billets originate from the difference in the thermomechanical path from the core to the billet surface and pose serious safety problems during further processing steps such as sawing the ingots. A thermomechanical model of continuous casting has been validated against residual stresses measured using neutron diffraction. The radial, hoop and axial stress components have been measured along the radius in a billet 320 mm in diameter.*

**Keywords:** continuous casting, aluminium alloys, internal stresses, neutron diffraction

## 1 Introduction

The fabrication of aluminum alloy extrusion products typically involves a number of steps starting from the semi-continuous casting of the cylindrical billet using a process known as direct chill (DC) casting and, depending on the alloy composition, ending with a post-extrusion heat treatment. Of the different processing stages, the casting process is particularly challenging since it gives rise to large thermally induced strains that can result in several types of casting defects including distortions, cracks, porosity, etc. Although these thermally induced strains can be partially relieved by permanent deformation, cracks will be generated either during solidification (hot tears) or post-solidification cooling (cold cracks) when stresses exceed the deformation limit of the alloy [1]. Furthermore, the thermally induced strains generally result in the development of large internal stresses within the billet after cooling to room temperature. These residual stresses will cause significant downstream processing and safety issues during the sawing stage prior to extrusion, when the billet is cut into section of about 1 m in length [2]. For large diameters (typically higher than 350 mm) and high-strength alloys (2xxx and 7xxx series), the residual stresses can lead to saw pinching first and then to crack initiation. In both cases, the elastic energy released upon sawing may cause personnel injury and equipment damage.

Currently, the most common technique for quantifying residual stresses that arise during manufacturing is through the use of numerical process models, generally using finite element (FE) mathematical techniques [3]. To be effective and accurate, these models require a significant understanding of the processing route and knowledge of the material's mechanical and physical behavior over a range of temperatures. The computation of stress evolution including billet distortions and residual stresses during the DC casting of aluminum alloys has been the scope of many studies since the late 1990's [3-9] and nowadays is a well-established technique. However, validation of these models, often done by comparing the computed and measured distortions at the billet surface, e.g. the butt-curl [7] and the rolling face pull-in for rolling

sheet ingots [8], remains challenging. Experimental validation against the computed room-temperature residual stresses is limited simply owing to the difficulty of measuring the internal strains in large castings and the high variability in the measurements. While some measurement techniques are available for quenching [10] or welding [11], they remain rare, uncertain, and are usually limited to only one or two components of the stress tensor near the surface of the casting [12,13]. In the past, destructive methods (hole-drilling [14], cut compliance [15]. etc.) have been used for measuring residual elastic strains. Physical methods such as X-ray, ultra-sound, or neutron diffraction (ND) have now become very attractive, since they can provide all of the components of the elastic strain tensor. With the development of powerful neutron beams, it is now possible to measure the residual elastic strains rather deep in light metal alloy systems such as aluminum and magnesium alloys since these metals are relatively transparent to neutrons. Such measurement allow for sophisticated model validation. In the current publication, residual strain measurements have been undertaken at POLDI [16] the Swiss neutron diffractometer located at PSI-Villigen and at SALSALSA [17], the neutron strain imager located at ILL-Grenoble, on the same AA6063 round billet section 160 mm in radius (R), 0.6 m in length and cast at 66 mm/min. The goal of the present paper is to present these measurements and to validate a thermomechanical finite element (FE) model of the DC casting process applied to cylindrical extrusion billets. This model is built in Abaqus and fully detailed in reference [18]. The minimum billet section-length necessary to maintain the distribution and magnitude of as-cast residual stresses was determined numerically. It was shown that this section-length has to be higher than three times the billet radius, 48 cm in the present study. The composition of the AA6063 alloy is 0.52 Si wt. pct., 0.60 Mg wt. pct. and 0.18 wt. pct. Fe. Its solidification interval is 557°C-655°C [18].

The FE model used to compute the residual stresses after casting showed that the stress tensor is diagonal in the (r,θ,z) cylindrical reference frame, thus reducing to three the number of unknown stress components. Section II provides a description of the principles of residual strain measurements using neutron diffraction. The residual stress measurements, along with a comparison of these results to the values predicted by the FE model, are provided in Section III. Finally the stored elastic energy is assessed in section IV.

## 2 Neutron Diffraction Measurements

### 2.1 Neutron Diffraction

POLDI and SALSALSA are neutron diffraction instruments designed for strain measurements through the accurate determination of lattice spacing. In a stressed material, the lattice spacing acts as a kind of strain gauge. If  $d_0$  and  $d$  are, respectively, the stress-free and actual lattice spacing for a given plane family, then the elastic strain is given by  $\varepsilon = (d-d_0)/d_0$ . Using Hooke's law, the measured strain can be converted to stress. The position of the diffraction peak intensity gives a measure of the average strain, whereas its width is related to strain fluctuations and to possible plastic deformation. Peak intensities can also provide information about texture. Diffraction can be understood in terms of the Bragg's law  $\lambda = 2d\sin\theta$  where  $d$  is the lattice spacing,  $\lambda$  the wavelength and  $2\theta$  the diffraction angle. Therefore in order to measure the lattice spacing for determining strains and stresses, either the wavelength is fixed and the diffraction angle is measured (monochromatic angular dispersive) or the diffraction angle is fixed and the wavelength determined (polychromatic time-of-flight). In the case of monochromatic where only one diffraction peak is recorded, for fcc metals such as aluminum, the (311) diffracting planes are commonly used to measure the strain since they do not accumulate significant intergranular stresses and hence exhibit similar behaviour as that of the bulk. The (311) is also recommended for use in the measurement of residual strains by neutrons in aluminium alloys by the ISO VAMAS standard [19]. This is the case of the measurements made on SALSALSA. In contrast, with the time of flight method, many diffraction peaks are measured corresponding to several families of lattice planes. Using a full pattern refinement, an average lattice parameter is determined from which strain and stress is subsequently calculated. With this method the range of elastic and plastic anisotropies are averaged, giving strain response akin to that of the bulk. This is the case with the POLDI measurements.

POLDI is a so-called time-of-flight instrument which means that the detector is placed at a fixed diffraction angle ( $90^\circ$ ) and that in contrast to monochromatic instruments a broad wave length spectrum is used. For the measurements at POLDI [16], a 3.8 mm collimator was used to define the sampling gauge volume. This rather large sample gauge volume ( $3.8 \times 3.8 \times 8 \text{ mm}^3$ ) gave reasonable measurement times, typically 2 hours per position per strain component. A series of stress free reference samples, for measurement of the reference lattice constant  $d_0$ , were also acquired. These samples were electro-discharge

machined along the billet radius every 20 mm in order to account for any variation in  $d_0$  with position within the billet that may be present due to long range chemical inhomogeneities, i.e. macrosegregation. Located at ILL-Grenoble, SALSA [17] uses a large crystal monochromator to select a particular neutron wavelength. The material to be studied is placed in this monochromatic neutron beam, and the scattered neutrons are collected on a large 2D detector to determine accurately the lattice spacing. The wavelength is constant (1.66 Å) and the position of the diffraction peak is recorded on a position sensitive detector. For the measurements at SALSA, 2 mm radial focusing collimators were used to reduce experimental errors introduced by the optics. A rather large instrumental gauge volume ( $2 \times 2 \times 15 \text{ mm}^3$ ), but with good lateral resolution in the scan direction, gave reasonable measurement times of on average 30 min. Again, a series of stress free reference samples, for measurement of the reference lattice constant  $d_0$ , were acquired.

## 2.2 Residual Strains and Stresses

In the DC casting process of billets, the elastic stress/strain tensor has only four components due to the axisymmetric billet geometry and casting conditions. Furthermore, since the billet section used for the residual strain measurements was taken from the central part or steady-state regime of casting, it can be assumed that this tensor depends only on radial position. This assumption was verified by the simulation results presented in [19]. FE calculations have also shown that the shear stress component of  $\sigma_{rz}$  is negligible thus further reducing the stress and strain tensors to three components, radial, hoop and axial. These tensors are therefore diagonal in the  $(r, \theta, z)$  reference frame and can be described by Hooke's law, where  $E$  is Young's modulus (71.3 GPa) and  $\nu$  the Poisson's ratio (0.3):

$$\begin{pmatrix} \sigma_r \\ \sigma_\theta \\ \sigma_z \end{pmatrix} = \frac{E}{(1+\nu)(1-2\nu)} \begin{pmatrix} 1-\nu & \nu & \nu \\ \nu & 1-\nu & \nu \\ \nu & \nu & 1-\nu \end{pmatrix} \begin{pmatrix} \varepsilon_r \\ \varepsilon_\theta \\ \varepsilon_z \end{pmatrix} \quad (1)$$

## 2.3 Beam path and billet position

For each of the three measured strain components, both the beam orientation and the position of the billet within the neutron chamber must be varied as presented in figure 1. For the radial component, the length of the beam path varies from almost zero at the billet surface to  $2R$  at the billet centre. For the axial component, the beam path remains near  $2\sqrt{2}R$  for each measurement, whereas for the hoop component, the beam path increases from  $\sqrt{2}R$  at the billet surface to  $2R$  at the billet centre. Obviously, count times for the axial measurements are the longest.

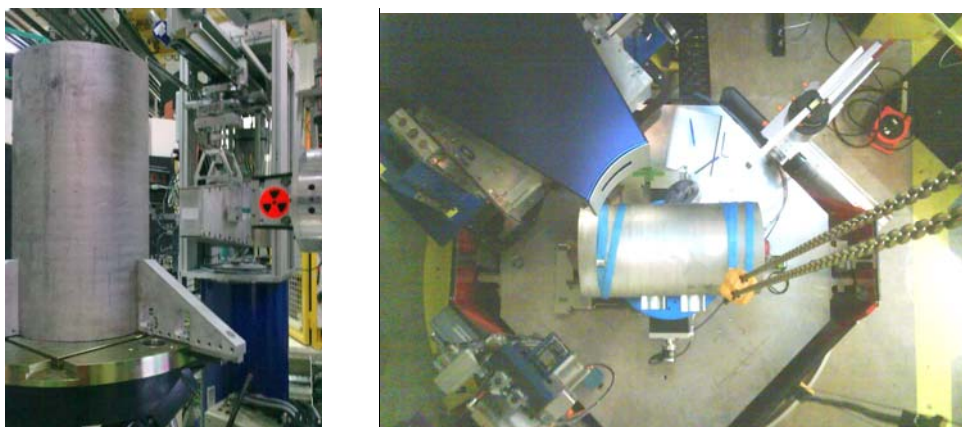


**FIG. 1:** billet section positioning for measuring the radial and hoop (left at Salsa) and axial (right at Poldi) strains. The weight of the billet sample is 130kg.

## 3 Measured and computed stress level

Residuals strains on a 0.6 m long AA6063 billet section, taken from the steady-state region of the casting, were measured at the two neutron diffractometers, POLDI and SALSA. The typical grain size in this

casting was 100 +/- 30 microns. As measuring time was reduced at Salsa owing to a higher neutron flux, roughly thirty two residual strain measurements were made along the radius of the billet in ~5 mm increments. Furthermore, since the AA6063 alloy was grain refined, no texture was present in the sample.

The radial distribution of the three stress components has been calculated at each radial position using Eq. 1. These stresses are shown in figures 2 to 4, along with the predicted stresses from the FE model. The error of the stress measurement is reported on each of the points using the elastic constants. The statistical error is larger for the axial stress at the billet centre owing to a longer beam path length, but still below 10 MPa. The centre of the billet is in tri-axial tension whereas its surface is in compression in the hoop and axial directions: these results are in full agreement with previous works [4-5] and are explained by the so-called skin-core effect [20]. Furthermore, the agreement between the stress components measured at SALSA and POLDI and the FE predictions is very good for all three components. The FE results always fall within the measured values except near the billet surface for the hoop stress and at the billet centre for the axial stress.

The locations where the axial and hoop stress components change sign are also very close to the measured ones. Note also that the measured radial stress component at the billet surface is -1.65 MPa at POLDI and 4 MPa at SALSA whereas it should be zero. This gives us an idea of the precision that can be obtained with such neutron measurements.

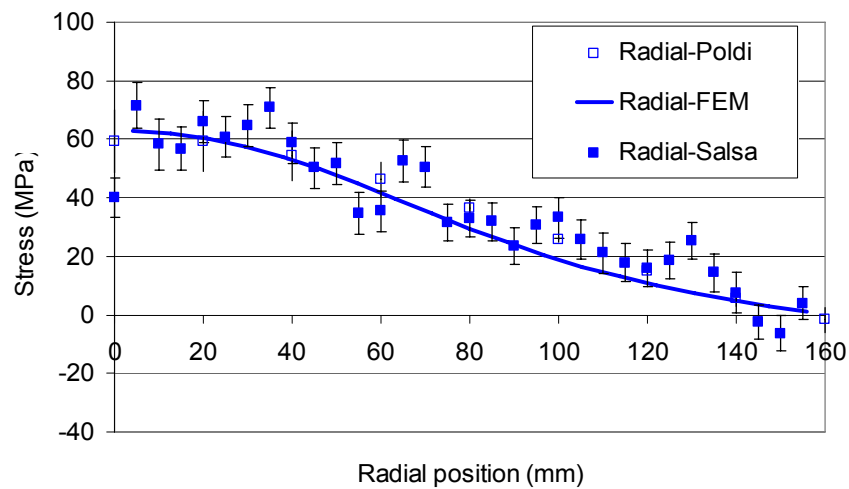


**FIG. 2:** comparisons between computed and measured radial stress component.

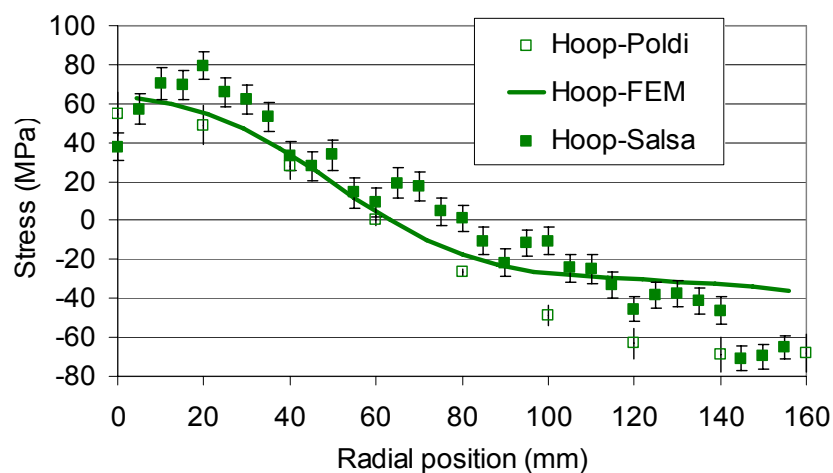


**FIG. 3:** comparisons between computed and measured hoop stress component.

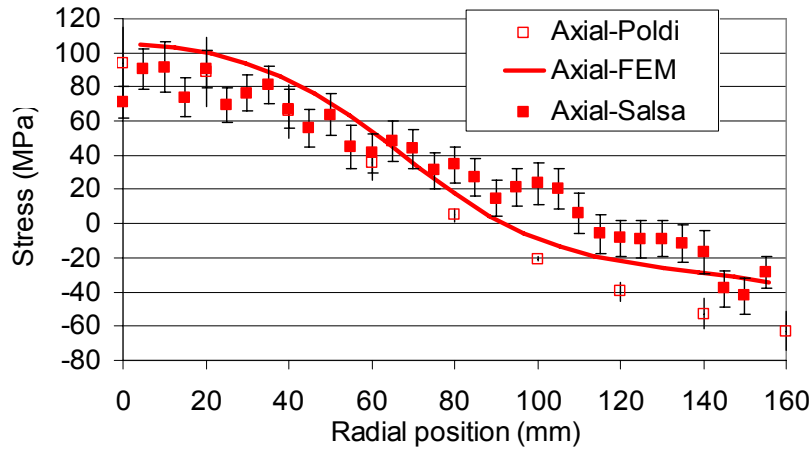


FIG.4: comparisons between computed and measured axial stress component.

#### 4 Stored elastic energy

The stored elastic energy in a billet section of length  $H$  and radius  $R$  is given by:

$$W = \int_V (\sigma:\varepsilon) dV = 2\pi H \int_0^R (\sigma_r \varepsilon_r + \sigma_\theta \varepsilon_\theta + \sigma_z \varepsilon_z) r dr \quad (2)$$

As the FE results fall within the measured values (cf. figures 2-4), the stored energy can be calculated using the FE predictions. Calculating integral (2) yields  $W/H = 2.4$  kJ/m for our billet sample ( $R=160$  cm). This leads to a volumetric stored elastic energy of  $29.6$  kJ/m<sup>3</sup>. The higher this value, the higher is the risk to get erratic dissipation of energy when sawing the billet [21]. In particular, this value increases with increasing casting speed thus limiting productivity. Casting recipes should be adapted in order to decrease this value. In addition, this stored energy is comparable to that found after quenching of 6xxx aluminum thick plates [22]. This can be explained by the fact that thermally induced deformations and associated stress build up are comparable in casting and in quenching.

#### 5 Conclusion

Prior to performing the residual stress measurements, the FE model of extrusion billet casting was first used to determine the minimum section-length which can be sawed from the billet without significantly relaxing the residual stresses at its mid-height. Based on the computation results, a billet section whose length exceeds three times the billet radius retains residual stresses which are similar in magnitude to the as-cast steady-state predicted value. Then, the as-cast residual stresses have been measured on a 0.6 m long steady-state section of an AA6063 DC cast extrusion billet using the neutron diffractometers POLDI and SALSA. The corresponding residual stresses indicate that while the billet centre is in high tri-axial tension, the billet skin is in bi-axial compression owing to the skin-core effect. This stress distribution is similar to the stress state encountered in quenching and welding. The measurements coming from POLDI and SALSA agree remarkably well. They have been used to validate the FE model of DC casting. Considering the numerous input parameters entering into the model (alloy properties, cooling conditions, etc.), the comparison between the measured and computed results is excellent and allows calculating the stored elastic energy that might dissipate erratically during sawing of the billet thus posing serious safety concerns. Further analysis of the diffraction peaks, notably its width, should allow us to determine the level of plastic deformation undergone by the alloy during casting.

#### 6 Acknowledgments

The authors express their acknowledgements to Alcan ATI Valais for providing the billet section on which neutron diffraction measurements have been carried out, the Institute Laue-Langevin in Grenoble (France) and the Swiss Neutron Source at PSI-Villigen for the provision of beam time.

## 7 References

- [1] W. Boender, A. Burghardht, E. P. van Klaveren, J. Rabenberg, *Numerical Simulation of DC casting, Interpreting the results of a Thermo-Mechanical Model*, Light Metals 2004, A. T. Tabereaux Ed., TMS, 2004, pp. 679-684.
- [2] Ludwig, J.-M. Drezet, B. Commet, B. Heinrich, *Modelling of Internal Stresses in DC casting and Sawing of High Strength Aluminum Alloys slabs*, in Modeling of Casting Welding and Advanced Solidification Processes, Eds. C.-A. Gandin and M. Bellet, pp. 185-192, Nice, 2006.
- [3] J.-M. Drezet, M. Rappaz, *Modelling of Ingot Distortions during Direct Chill Casting of Aluminium Alloys*, Met. Mat. Trans. A, **27A**, 1996, pp. 3214-3225.
- [4] B. Hannart, F. Cialti, R. V. Schalkwijk, *Thermal Stresses in DC Casting of Aluminum Slabs: Application of a Finite Element Model*, Light Metals 1994, A. T. Tabereaux Ed., TMS, 1994, pp. 879-887.
- [5] H. Fjaer and A. Mo: Alspen: a mathematical model for thermal stresses in direct chill casting of aluminium billets, Met. Mat. Trans. A, **21B**, 1990, pp. 1049-1061.
- [6] J. Sengupta, S.L. Cockcroft, D.M. Maijer, A. Larouche, *Quantification of temperature, stress, and strain fields during the start up phase of DC casting process by using a 3D fully coupled thermal and stress model for AA5182 ingots*, Mat. Sc. Eng A, **397**, 2005, pp. 157-177.
- [7] W. Droste, J.-M Drezet, G.-U Gruen and W. Schneider: 3D Modeling of Ingot Geometry Development of DC-cast Aluminium Ingots during the Start-up Phase, in Continuous Casting, Eds: K. Ehrke and W. Schneider, DGM, Wiley-VCH, Frankfurt 2000, pp. 175-183.
- [8] W. Droste, G.-U Grün, W. Schneider and J.-M. Drezet.: Thermo-Mechanical Modeling to Predict Shrinkage, Shape and Mold Openings for DC-Cast Rolling Ingots, in Light Metals, Eds. Wolfgang Schneider, TMS 2002, Seattle, pp. 703-708.
- [9] K. Escobar et al.: On the residual stress control in aluminium alloys 7050, Materials Science Forum vols. 396-402 (2002), p. 1235-1240.
- [10] D. Bru, J. Devaux, J.M. Bergheau and D. Pont: Mathematical Modeling of Weld Phenomena 3, H. Cerjak, ed., The Institute of Metals, Graz, AUS, 1997, pp. 456-63.
- [11] S. Ganguly, M. E. Fitzpatrick and L. Edwards: Comparative neutron and synchrotron X-ray diffraction studies to determine residuals stress on an as-welded AA2024 plate, Materials Science Forum vols. 790-491 (2005), pp. 223-228.
- [12] J. Moriceau: Thermal stresses in continuous DC casting of Al alloys, discussion of hot tearing mechanisms, Light Metals (TMS), 1975, p. 119-133
- [13] S. A. Levy et al.: Residual stress measurements for studying ingot cracking, Light Metals (TMS), 1974, p. 571-585.
- [14] J. Lu, *Handbook of Measurement of residual stresses*, Society for Experimental Mechanics, Inc. The Fairmont Press, Ed. J. Lu, 1996.
- [15] H. Hao, D.M. Maijer, M.A. Wells, S.L. Cockcroft and R.B. Rogge, "Prediction and measurement of residual stresses/strains in a direct chill casting magnesium alloy billet," *Magnesium Technology*, (2005), 223-228.
- [16] Poldi, Pulse overlap time-of-flight diffractometer, POLDI, Paul Scherrer Institut, Villigen, Switzerland, <http://poldi.web.psi.ch/>
- [17] Salsa, Strain imager for engineering applications SALSA, Institut Laue Langevin, Grenoble, France <http://www.ill.eu/instruments-support/instruments-groups/instruments/salsa/>
- [18] J.-M. Drezet and A. Phillion: As-cast residual stresses in an aluminum alloy AA6063 billet: neutron diffraction measurements and finite element modelling, in Met. and Mat. Trans. Vol. 41 A, pp. 3396-3404, December 2010.
- [19] G.A. Webster: VAMAS TWA 20 standard. Technical report, International Organisation for Standardisation (ISO), 2001.
- [20] J.-M. Drezet and M. Rappaz, *Ingot Distortions and Residual Stresses in Direct Chill Casting of Aluminium Alloys* in Proceedings of the 4th European Conference on Residual Stresses, ECRS 1996, SF2M, Eds. S. Denis et al., Cluny, France, pp. 357-366.
- [21] J.-M. Drezet, O. Ludwig, C. Jaquerod and E. Waz: Fracture prediction during sawing of DC cast high strength aluminium alloy rolling slabs, in Inter. Journal of Cast Metals, 2007, vol. 20, no. 3, p. 163-170.
- [22] F. Heymès, B. Commet, B. Dubost, P. Lassince, P. Lequen and G.M. Reynaud, *Development of new Al Alloys for distortion free machined aluminum aircraft components*, 1<sup>st</sup> International Non-ferrous Processing and Technology Conference, St Louis, Missouri, 10-12 march 1997.